BMC Pharmacology and Toxicology

RESEARCH

Open Access

Identification of benzo(a)pyrene-related toxicological targets and their role in chronic obstructive pulmonary disease pathogenesis: a comprehensive bioinformatics and machine learning approach

Jiehua Deng[1], Lixia Wei[1,2*], Yongyu Chen[3], Xiaofeng Li[4], Hui Zhang[4], Xuan Wei[4], Xin Feng[5], Xue Qiu[2], Bin Liang[6] and Jianquan Zhang[1*]

Abstract

Background Chronic obstructive pulmonary disease (COPD) pathogenesis is influenced by environmental factors, including Benzo(a)pyrene (BaP) exposure. This study aims to identify BaP-related toxicological targets and elucidate their roles in COPD development.

Methods A comprehensive bioinformatics approach was employed, including the retrieval of BaP-related targets from the Comparative Toxicogenomics Database (CTD) and Super-PRED database, identification of differentially expressed genes (DEGs) from the GSE76925 dataset, and protein-protein interaction (PPI) network analysis. Functional enrichment and immune infiltration analyses were conducted using GO, KEGG, and ssGSEA algorithms. Feature genes related to BaP exposure were identified using SVM-RFE, Lasso, and RF machine learning methods. A nomogram was constructed and validated for COPD risk prediction. Molecular docking was performed to evaluate the binding affinity of BaP with proteins encoded by the feature genes.

Results We identified 72 differentially expressed BaP-related toxicological targets in COPD. Functional enrichment analysis highlighted pathways related to oxidative stress and inflammation. Immune infiltration analysis revealed significant increases in B cells, DC, iDC, macrophages, T cells, T helper cells, Tcm, and TFH in COPD patients compared to controls. Correlation analysis showed strong links between oxidative stress, inflammation pathway scores, and the infiltration of immune cells, including aDC, macrophages, T cells, Th1 cells, and Th2 cells. Seven feature genes (ACE, APOE, CDK1, CTNNB1, GATA6, IRF1, SLC1A3) were identified across machine learning methods. A nomogram based on these genes showed high diagnostic accuracy and clinical utility. Molecular docking revealed the highest binding affinity of BaP with CDK1, suggestive of its pivotal role in BaP-induced COPD pathogenesis.

*Correspondence:
Lixia Wei
weilx004011@aliyun.com
Jianquan Zhang
jqzhang2002@126.com

Full list of author information is available at the end of the article

Conclusions The study elucidates the molecular mechanisms of BaP-induced COPD, specifically highlighting the role of oxidative stress and inflammation pathways in promoting immune cell infiltration. The identified feature genes may serve as potential biomarkers and therapeutic targets. Additionally, the constructed nomogram demonstrates high accuracy in predicting COPD risk, providing a valuable tool for clinical application in BaP-exposed individuals.

Keywords Chronic obstructive pulmonary disease, Bioinformatics, Immune score, KEGG, Benzo(a)pyrene, Polycyclic aromatic hydrocarbons

Introduction

Chronic obstructive pulmonary disease (COPD) is a progressive and debilitating respiratory condition characterized by persistent airway inflammation and obstruction, affecting millions of people worldwide [1]. COPD is a leading global cause of death, and its prevalence is projected to increase, highlighting the urgent need for further research in this area [2, 3]. The pathogenesis of COPD is multifactorial, involving genetic predispositions and environmental exposures [4]. Among the environmental factors, the polycyclic aromatic hydrocarbon commonly found in tobacco smoke, vehicular emissions, and industrial pollutants, has garnered significant attention due to its potential role in COPD [5].

Benzo(a)pyrene (BaP), a major polycyclic aromatic hydrocarbon, is commonly identified in terrestrial soils, surface water bodies, atmospheric air, and sedimentary deposits. This compound is present in tobacco smoke and various food items, particularly those subjected to smoking or grilling processes, resulting in widespread human exposure. An increasing volume of research underscores the hazardous effects associated with this substance [6]. Previous studies have established a connection between environmental pollutants, including polycyclic aromatic hydrocarbon, and the onset and exacerbation of COPD [5, 7–9]. BaP is known to exert its toxicological effects through the generation of reactive oxygen species (ROS) and the activation of inflammatory pathways [10, 11]. While several investigations have identified genetic and molecular contributors to COPD, the specific toxicological targets of BaP in COPD pathogenesis remain underexplored [12, 13]. Existing research has highlighted the need for comprehensive analyses integrating bioinformatics and machine learning techniques to elucidate the complex interactions between BaP exposure and COPD.

The motivation behind this research stems from the critical necessity to understand the molecular mechanisms underlying BaP-induced COPD. By identifying and characterizing the toxicological targets of BaP, we aim to uncover novel biomarkers and therapeutic targets, potentially transforming the diagnosis and treatment strategies for COPD patients exposed to environmental pollutants. This study distinguishes itself by employing an innovative, multilayered bioinformatics strategy that not only integrates traditional analysis with advanced machine learning methodologies but also introduces new conceptual frameworks for understanding BaP-related toxicological effects. This approach underscores the interconnectedness of oxidative stress, inflammation, and immune cell infiltration, providing unique insights into COPD pathogenesis.

The primary objective of this study is to identify BaP-related toxicological targets and elucidate their roles in the development of COPD. To achieve the objective, we employed a comprehensive bioinformatics approach. BaP-related targets were retrieved from the Comparative Toxicogenomics Database (CTD) and Super-PRED database, while DEGs were identified from the GSE76925 dataset. We performed PPI network analysis to explore the interactions among identified targets. Functional enrichment and immune infiltration analyses were conducted using GO, KEGG, and ssGSEA algorithms. Machine learning methods, including SVM-RFE, Lasso, and Random Forest (RF), were utilized to identify BaP-related feature genes. A nomogram was constructed and validated based on the identified feature genes for COPD risk prediction. Finally, molecular docking was carried out to assess the binding affinity of BaP with the feature gene-encoded proteins.

This study elucidates the molecular mechanisms of BaP-induced COPD, specifically highlighting the roles of oxidative stress and inflammation pathways in promoting immune cell infiltration. The identified feature genes may serve as potential biomarkers and therapeutic targets, offering new avenues for COPD diagnosis and treatment. Additionally, the constructed nomogram, demonstrating high diagnostic accuracy, provides a valuable tool for predicting COPD risk in BaP-exposed individuals, with significant implications for clinical practice and public health.

Methods

Data acquisition and preprocessing

We acquired the dataset GSE76925 and GSE38974, relevant to COPD, from the NCBI Gene Expression Omnibus (GEO) database. The GSE76925 dataset consists of 44 control (Con) samples and 111 COPD samples, serving as the training set. The GSE38974 dataset includes 9 Con samples and 23 COPD samples, utilized as the validation set (Table S1). The raw matrix files were extracted and normalized using the Affy package. To convert probe data to gene symbols, we utilized the annotation file from

the GPL10558 platform. For genes associated with multiple probes, the mean value of the probes was used as the gene expression value. Genes and samples with more than 50% missing values were removed from further analysis. For the remaining missing values, we used the impute package in R, employing the K-nearest neighbors method with K set to 10. Subsequently, median normalization was performed to standardize expression levels across the dataset. DEGs between the Con group and the COPD group were identified using the limma package. Genes with an adjusted P-value of less than 0.05 were considered significantly differentially expressed.

Collection of BaP-related targets

We collected a list of genes associated with both COPD and BaP exposure using the CTD (http://ctdbase.org/). Additionally, we predicted BaP-related targets using the Super-PRED database (https://prediction.charite.de/index.php). The target genes from both datasets were integrated, and duplicate target genes were removed to obtain a list of BaP target genes.

Protein-protein interaction (PPI) network and enrichment analysis

To identify common genes between DEGs and BaP-related targets, we used the Venny tool. These common genes were designated as differentially expressed BaP-related toxic genes. We constructed a PPI network for these toxic genes using the STRING database (https://string-db.org/), with a confidence threshold set at 0.7. The network visualization was performed using Cytoscape software. For Gene Ontology (GO) functional annotation and Kyoto Encyclopedia of Genes and Genomes (KEGG) pathway enrichment analysis of the toxic genes, we used the clusterProfiler and enrichplot packages. A threshold of adjusted P-value less than 0.05 was set for statistical significance.

Immune cell infiltration analysis

To assess the levels of 24 immune cell subtypes within the samples, we employed single-sample Gene Set Enrichment Analysis (ssGSEA). The gene sets used to evaluate the enrichment levels of different immune cell subtypes were obtained from a previous study by Han et al. [14]. Using the GSVA algorithm, we calculated the oxidative stress and inflammation signaling pathway scores for each sample. Pearson correlation analysis was then performed to determine the correlation between the characteristic pathway scores and the immune cell components.

Machine learning

To identify key toxic targets, we utilized three machine learning models: Random Forest (RF), Least Absolute Shrinkage and Selection Operator (LASSO) regression, and Support Vector Machine-Recursive Feature Elimination (SVM-RFE). We implemented the Random Forest algorithm using the randomForest package in R, which constructs multiple decision trees and ranks the importance of each feature based on the mean decrease in accuracy or the Gini index. We constructed a forest of 500 decision trees, with the number of trees determined through cross-validation to ensure stability. We also optimized the model parameters, including the maximum depth of the trees and the minimum sample size at leaf nodes, using a grid search method. LASSO regression was performed using the glmnet package in R, applying L1 regularization to shrink some coefficients to zero and effectively selecting significant features. The optimal lambda was determined through a 10-fold cross-validation process aimed at minimizing the mean squared error. SVM-RFE was executed with the e1071 package in R, recursively eliminating the least important features based on their weights within a support vector machine classifier to rank the features by importance. For SVM-RFE, we employed a radial basis function kernel, and the hyperparameters, including the penalty parameter C and the kernel coefficient gamma, were optimized using a grid search coupled with 5-fold cross-validation. The results from the RF, LASSO, and SVM-RFE models were integrated using the Venny tool to identify common important toxic targets.

Construction of artificial neural network (ANN) model

Using the Neural Networks R package, an ANN model was developed to examine 7 key genes identified by machine learning. The expression levels of these genes were converted into gene labels, and their expression levels were compared to the median expression levels across all samples. For genes that were upregulated, a value of 1 was assigned if the expression was above the median, otherwise, it was assigned a value of 0. Conversely, for down-regulated genes, a value of 0 was assigned if the expression level exceeded the median, and 1 otherwise. A gene tag table was then constructed, setting the ANN hidden layer size to 4 to derive the gene weights from the gene labels. Utilize the Receiver Operating Characteristic (ROC) curve to assess the predictive efficacy of the ANN within both the training and validation datasets.

Development of nomogram

To construct and evaluate the nomogram, we integrated the core toxic genes using the rms package in R. The nomogram was developed to predict the likelihood of COPD. To assess its predictive capability, we performed a Receiver Operating Characteristic (ROC) curve analysis, which provided insights into the model's sensitivity and specificity. Additionally, a calibration curve analysis was conducted to evaluate the accuracy of the nomogram by

comparing predicted probabilities with actual outcomes. To further assess the clinical utility and net benefit of the nomogram across different probability thresholds, we carried out a decision curve analysis.

Molecular docking

To examine the interactions between small molecule compounds and core toxic target proteins, we executed a molecular docking analysis. Small molecule compounds were retrieved from the PubChem database in SDF format. These files were transformed into PDBQT format using AutoDock Tools for the docking process. The three-dimensional structures of the target proteins were obtained from the Protein Data Bank (https://www.rcsb.org). We prepared these protein structures by removing water molecules, adding hydrogen atoms, and assigning the correct charges with AutoDock Tools. AutoDock was then used to conduct the docking analysis, predicting the binding affinities and interaction patterns between the small molecules and the target proteins. We analyzed the docking results based on binding energy scores to determine the most favorable binding sites. The interactions between the ligands and the target proteins were visualized using PyMOL software (version 1.0.0).

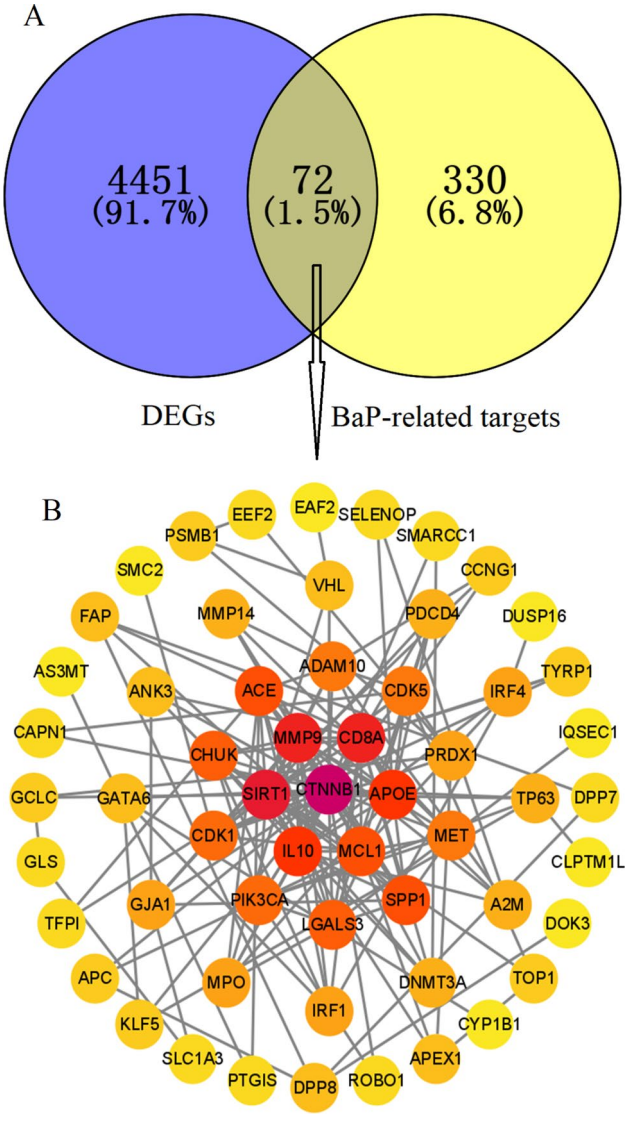

Fig. 1 Identification and interaction analysis of differentially expressed benzo(a)pyrene-related targets in COPD. **A** Venn diagram showing the intersection of DEGs in COPD from the GSE76925 with benzo(a)pyrene-related targets obtained from the Comparative Toxicogenomics Database and Super-PRED database. **B** PPI network analysis of the 72 differentially expressed benzo(a)pyrene-related toxicological targets. Each node represents a gene, and edges represent the interactions between them. The color intensity of the nodes indicates the degree of connectivity, with redder nodes having higher connectivity

Results

Identification of differentially expressed benzo(a)pyrene-related toxicological targets in COPD.

A total of 402 benzo(a)pyrene-related targets were retrieved from the Comparative Toxicogenomics Database (CTD) and Super-PRED database, while 4523 differentially expressed genes (DEGs) associated with chronic obstructive pulmonary disease (COPD) were identified from the GSE76925 dataset. The intersection of benzo(a)pyrene-associated targets and DEGs yielded 72 differentially expressed benzo(a)pyrene-related toxicological targets (Fig. 1A). We performed a protein-protein interaction (PPI) network analysis on the 72 differentially expressed benzo(a)pyrene-related toxicological targets to understand their interconnections and potential biological implications. The PPI network, presented in Fig. 1B, highlights a central cluster of targets, including highly connected nodes such as MMP9, CD8A, IL10, SIRT1, CTNNB1, and APOE, suggesting their significant roles in the pathogenesis of COPD influenced by benzo(a)pyrene exposure.

Functional enrichment analysis

As shown in Fig. 2A, GO enrichment analysis was performed on the 72 differentially expressed Benzo(a)pyrene-related toxicological targets in the context of biological processes (BP), cellular components (CC), and molecular functions (MF). The significant terms in the BP category included response to oxidative stress, response to reactive oxygen species, and cellular response to chemical stress. In the CC category, significant terms such as lamellipodium, lateral plasma membrane, and melanosome were identified. For the MF category, serine hydrolase activity, serine-type peptidase activity, and catalytic activity were among the enriched terms. As shown in Fig. 2B, KEGG pathway enrichment analysis identified several pathways significantly associated with the differentially expressed benzo(a)pyrene-related targets. Key pathways included MicroRNAs in cancer, Alzheimer

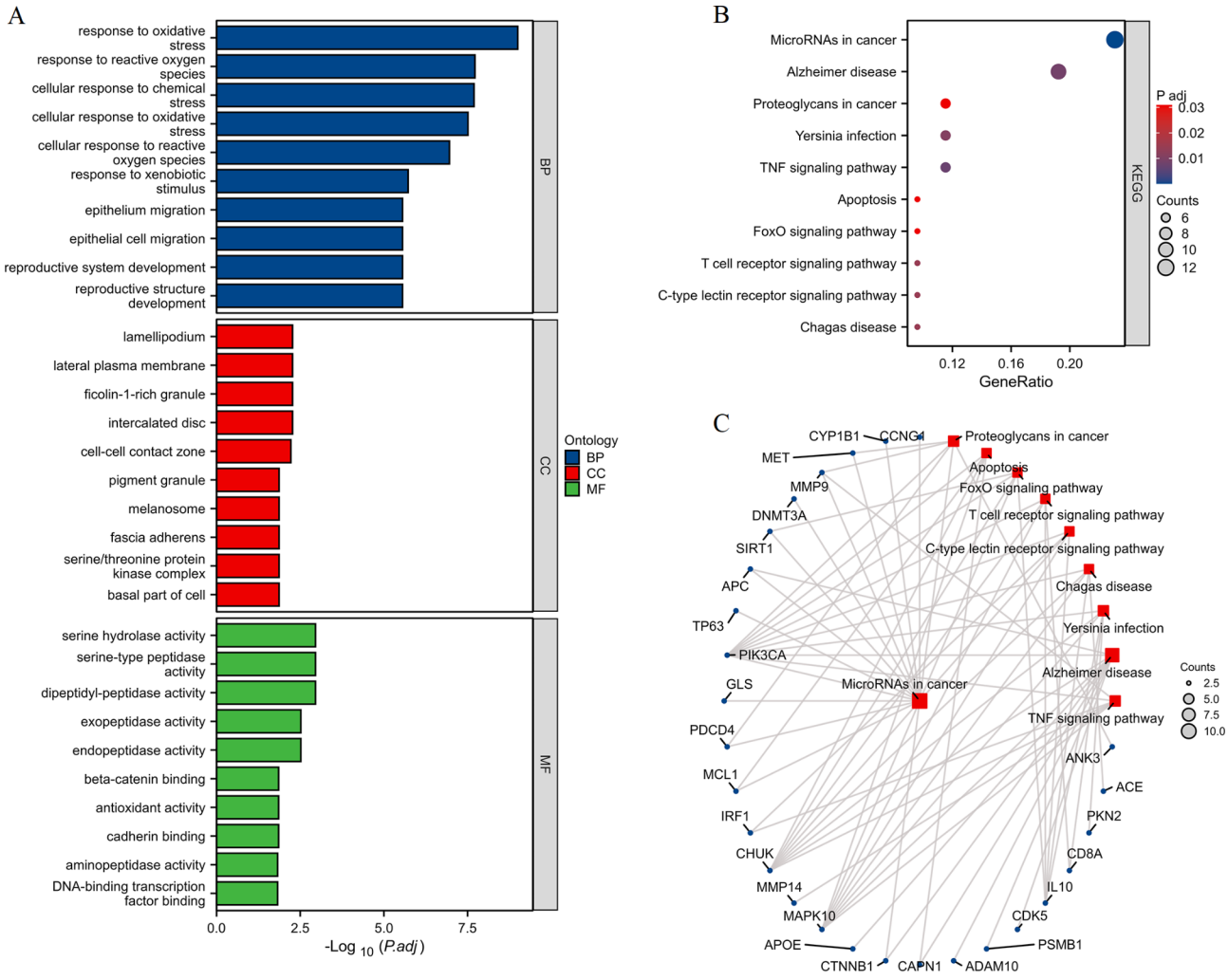

Fig. 2 Functional and pathway enrichment analysis of differentially expressed benzo(a)pyrene-related targets in COPD. **A** GO enrichment analysis of the 72 differentially expressed benzo(a)pyrene-related targets, categorized into biological processes (BP), cellular components (CC), and molecular functions (MF). The x-axis represents the -log10 adjusted p-value, indicating the significance of enrichment. **B** KEGG pathway enrichment analysis displaying the significant pathways identified. The x-axis shows the gene ratio, and the color gradient represents the adjusted p-value, with bubble size indicating the number of genes involved. **C** Network representation of significant KEGG pathways and their associated genes. Nodes represent genes, and edges denote their involvement in specific pathways. Pathways are marked as red squares, with the size of the squares indicating the number of associated genes

disease, Proteoglycans in cancer, and TNF signaling pathway. A network representation of the significant KEGG pathways and their associated genes was constructed (Fig. 2C). Key nodes representing pathways such as MicroRNAs in cancer, FoxO signaling pathway, and TNF signaling pathway were identified, with links illustrating the involvement of specific genes in multiple pathways. For instance, pivotal genes like PIK3CA, CHUK, MAPK10, and IL10 were found to be central within this network, underscoring their potential roles in toxicity mechanisms related to benzo(a)pyrene exposure in COPD. A Sankey bubble plot was constructed to visualize the enrichment of pathways associated with oxidative stress and inflammation in the context of differentially expressed benzo(a)pyrene-related toxicological targets (Fig. 3). The plot illustrates the connections between the identified genes (left) and their corresponding enriched pathways (right). Major pathways such as TNF signaling pathway, C-type lectin receptor signaling pathway, T cell receptor signaling pathway, and FoxO signaling pathway are prominently involved in inflammatory responses. Simultaneously, pathways including response to oxidative stress, response to reactive oxygen species, cellular response to chemical stress, and response to xenobiotic stimulus highlight the significant role of oxidative stress. The integration of these data underscores the importance of oxidative stress and inflammatory signaling pathways in the toxicological impact of benzo(a)pyrene in COPD, highlighting potential therapeutic targets and mechanisms.

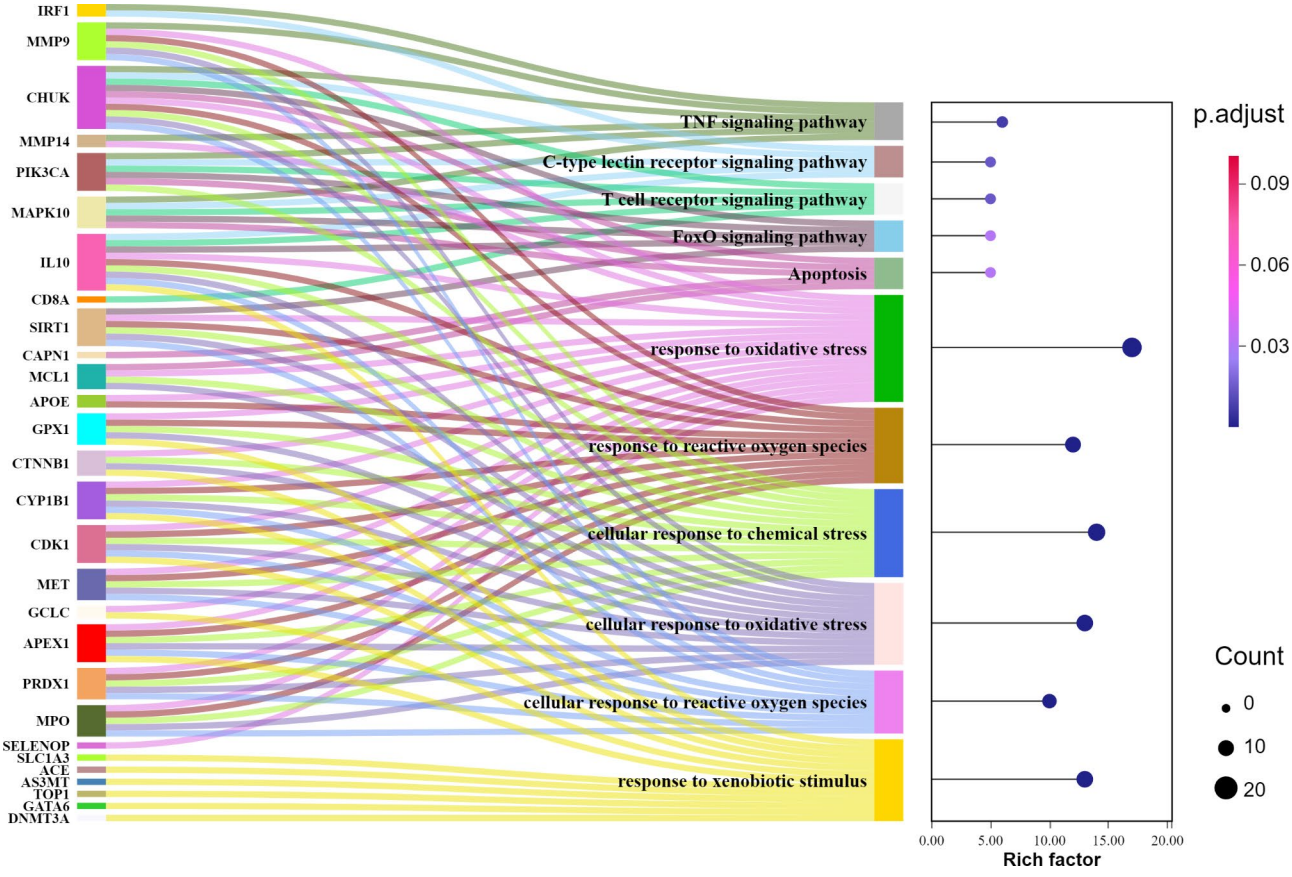

Fig. 3 Sankey bubble plot of enriched pathways related to oxidative stress and inflammation. This figure illustrates the relationships between differentially expressed benzo(a)pyrene-related toxicological targets and their enriched pathways associated with oxidative stress and inflammation. On the left, individual genes are listed, while the pathways they are involved in are shown on the right. The bubble plot on the right quantifies pathway enrichment, with the x-axis representing the rich factor and bubble size indicating the number of genes involved in each pathway. The color gradient represents the adjusted p-value, with darker colors indicating higher significance

Assessment of immune cell infiltration

ssGSEA was employed to evaluate the levels of immune cell infiltration in the Con and COPD groups. As shown in Fig. 4A, the infiltration levels of B cells, DC, iDC, macrophages, T cells, T helper cells, Tcm, and TFH were significantly elevated in the COPD group compared to the control group ($p < 0.05$). The heatmap illustrates the ssGSEA scores of various immune cell subpopulations across all samples (Fig. 4B). It clearly reveals the differing patterns of immune cell infiltration found in COPD patients compared to healthy individuals. These findings suggest substantial alterations in immune cell landscapes in COPD, providing insights into the immunological mechanisms underlying disease pathogenesis and potential targets for therapeutic interventions.

Evaluation and correlation of oxidative stress and inflammation pathway scores with immune cell infiltration

The ssGSEA algorithm was utilized to compare the GSVA scores of oxidative stress and inflammation signaling pathways between the Con and COPD groups (Fig. 5A). The violin plots illustrate a significant increase in the scores for both the response to reactive oxygen species and TNF signaling pathway in the COPD group compared to the Con group ($p < 0.05$). The heatmap displays ssGSEA scores stratified into low and high groups based on response to reactive oxygen species pathway scores (Fig. 5B). Notably, this pathway scores were positively correlated with the infiltration levels of aDC ($R = 0.409$, $p < 0.001$), DC ($R = 0.299$, $p < 0.001$), macrophages ($R = 0.475$, $p < 0.001$), neutrophils ($R = 0.305$, $p < 0.001$), T cells ($R = 0.422$, $p < 0.001$), T helper cells ($R = 0.285$, $p < 0.001$), Tcm ($R = 0.313$, $p < 0.001$), Th1 cells ($R = 0.495$, $p < 0.001$), and Th2 cells ($R = 0.338$, $p < 0.001$), indicating a significant association between oxidative stress and enhanced immune infiltration in COPD. Similarly, the correlation between the TNF signaling pathway score and immune cell infiltration levels was assessed (Fig. 5C). The heatmap shows a positive correlation with key immune cell types, including aDC ($R = 0.405$, $p < 0.001$), macrophages ($R = 0.313$, $p < 0.001$), T cells ($R = 0.502$, $p < 0.001$), T helper cells ($R = 0.289$, $p < 0.001$), Th1 cells ($R = 0.554$,

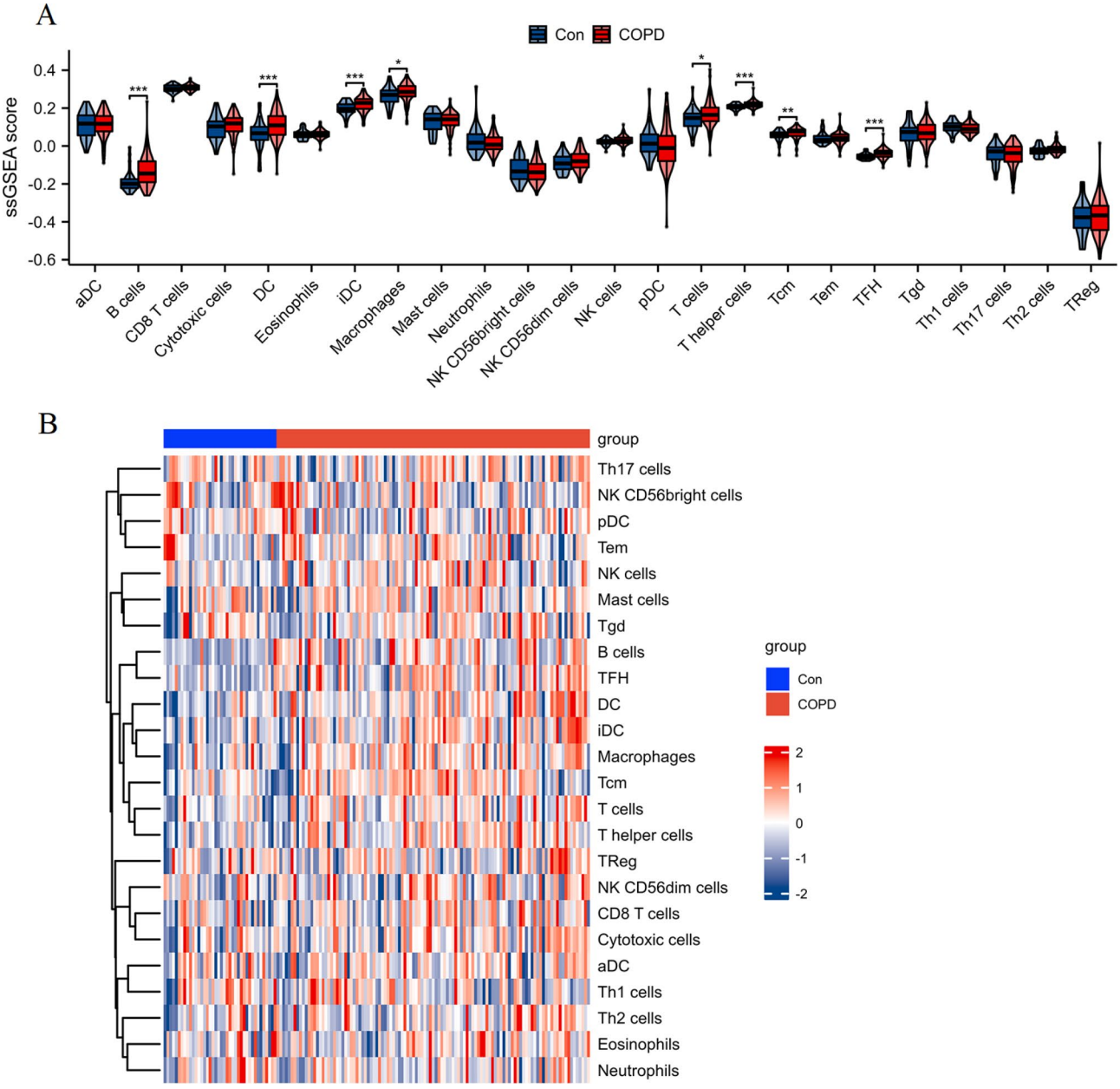

Fig. 4 Evaluation of immune cell infiltration levels between control and COPD groups. **A** Violin plots depicting the ssGSEA scores for various immune cell types in Con and COPD groups. Statistical significance is indicated as follows: *$p < 0.05$, **$p < 0.01$, ***$p < 0.001$. **B** Heatmap representing the ssGSEA scores of immune cell subpopulations across individual samples in the control and COPD groups. Rows correspond to different immune cell types, and columns represent individual samples. The color gradient denotes the infiltration levels, with red indicating higher and blue indicating lower scores

$p < 0.001$), and Th2 cells ($R = 0.313$, $p < 0.001$). These findings highlight the involvement of TNF signaling in promoting immune cell infiltration within the COPD environment. In summary, the significantly elevated scores for oxidative stress and inflammation pathways in the COPD group, along with their strong correlations with increased immune cell infiltration, underscore the critical role of these signaling events in the pathogenesis of COPD induced by benzo(a)pyrene exposure.

Identification of benzo(a)pyrene exposure-related signature genes using machine learning

As shown in Fig. 6A, SVM-RFE was employed to identify feature genes based on oxidative stress and inflammation-related gene expression profiles. The plot shows the 5-fold cross-validation accuracy against the number of features, with the maximal accuracy rate of 0.84 achieved using 25 features. Lasso regression was used to select feature genes. The plot presents the binomial deviance as a function of Log(λ), with the optimal λ determined

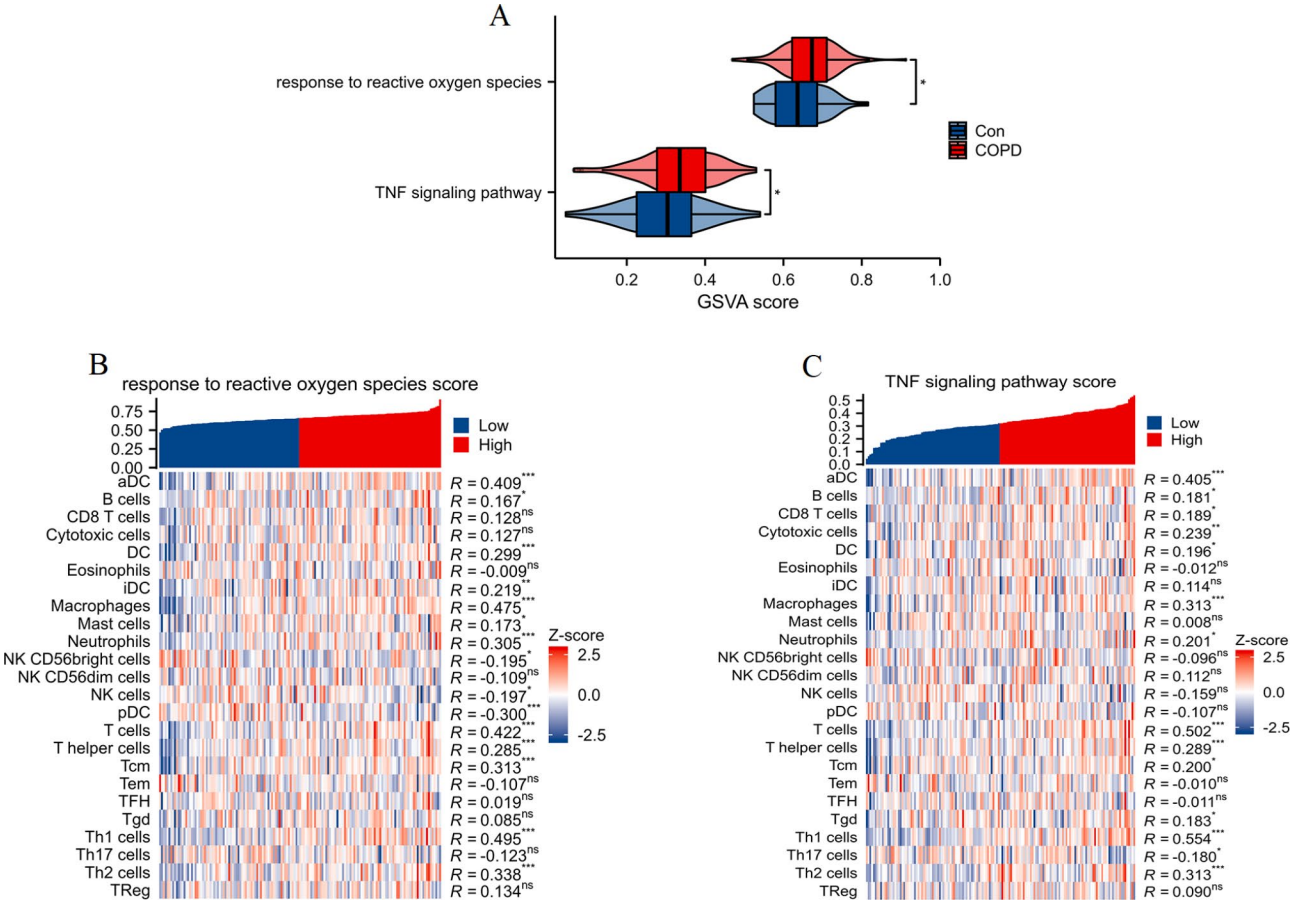

Fig. 5 Evaluation of oxidative stress and inflammation signaling pathways. **A** Violin plots comparing the scores of the response to reactive oxygen species and TNF signaling pathway between the Con and COPD groups using the ssGSEA algorithm. **B** Correlation of response to reactive oxygen species scores with immune cell infiltration. **C** Correlation of TNF signaling pathway scores with immune cell infiltration. The color gradient in the heatmaps represents the Z-scores of immune cell infiltration, with red indicating higher and blue indicating lower levels. The correlation coefficient (R) values and significance levels are denoted alongside each cell type. Statistical significance is indicated as follows: $*p < 0.05$, $**p < 0.01$, $***p < 0.001$

by the minimum deviance (Fig. 6B). RF algorithm was used to rank the importance of genes in distinguishing COPD patients. The bar graph displays the top feature genes ranked by the mean decrease in Gini coefficient, with CTNNB1, APOE, and SLC1A3 among the highest-ranked (Fig. 6C). Venn diagram illustrating the overlap of feature genes identified by the three machine learning methods (SVM-RFE, Lasso, and RF). A common set of 7 feature genes was identified across all methods: ACE, APOE, CDK1, CTNNB1, GATA6, IRF1, and SLC1A3 (Fig. 6D). Violin plots depicting the expression levels of the common feature genes between the Con and COPD groups in the GSE76925 dataset (Fig. 6E). Significant differences ($p < 0.001$) were observed for all these genes, with APOE and SLC1A3 showing increased expression, and ACE, CDK1, CTNNB1, GATA6, and IRF1 showing decreased expression in the COPD group. To evaluate the diagnostic efficacy of the predictive model, the GSE38974 dataset was utilized for external validation. The genes identified through three distinct supervised machine learning algorithms were employed for the receiver operating characteristic (ROC) analysis. The findings indicated an area under the curve (AUC) of 0.884 for the GSE38974 dataset (Figure S1). These machine learning analyses underscore the robustness of the identified feature genes, which may serve as biomarkers for benzo(a) pyrene exposure and contribute to understanding the molecular mechanisms underlying COPD pathogenesis.

Construction and validation of a nomogram for COPD risk prediction

A nomogram was constructed based on the expression profiles of the seven identified feature genes (ACE, APOE, CDK1, CTNNB1, GATA6, IRF1, SLC1A3) to predict the risk of COPD in patients exposed to benzo(a) pyrene (Fig. 7A). Each gene's expression level is assigned a score, and the total score corresponds to a linear predictor for the probability of COPD. The ROC curve of the nomogram model demonstrates an area under the curve (AUC) of 0.899, indicating high diagnostic accuracy

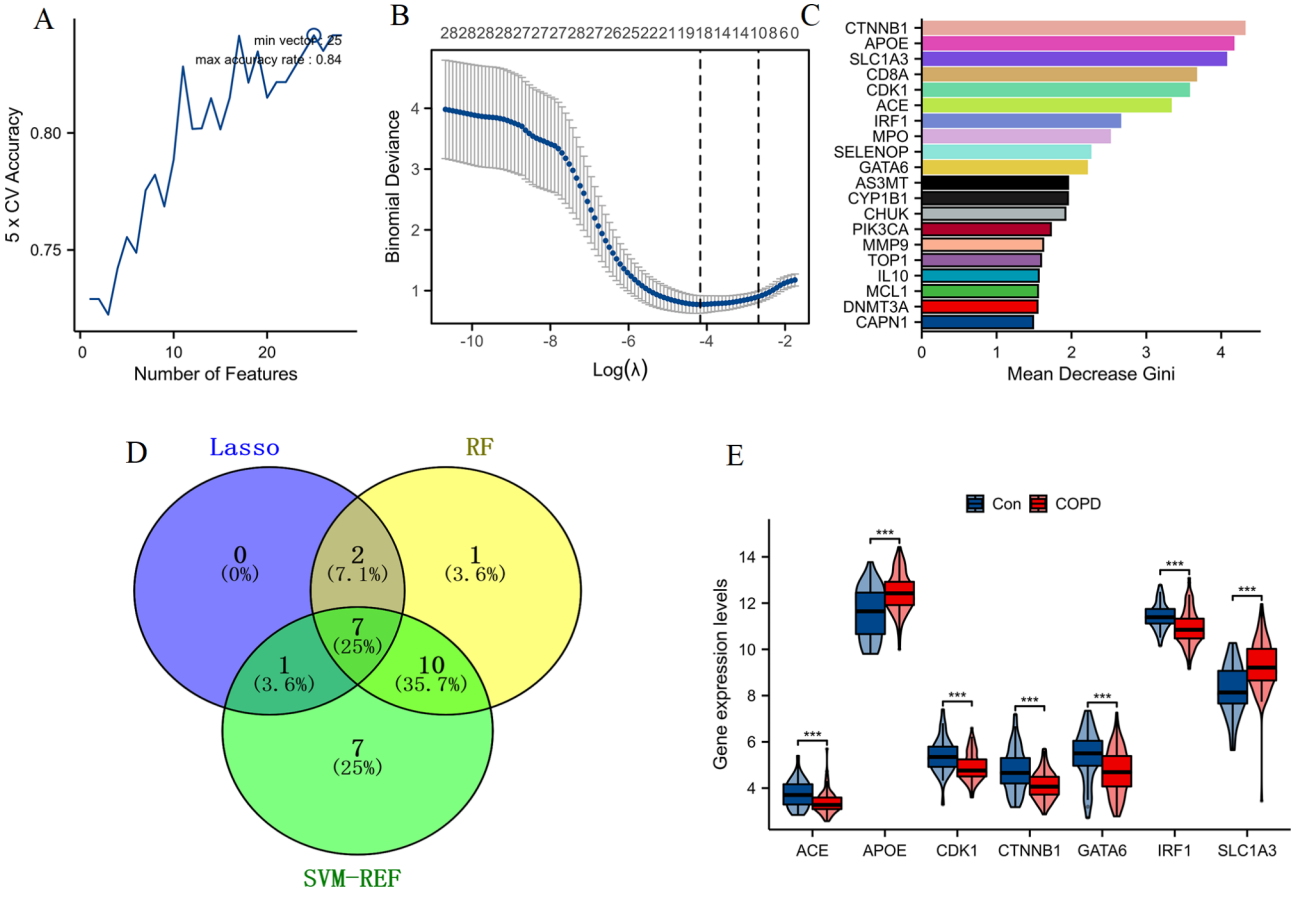

Fig. 6 Identification of benzo(a)pyrene exposure-related feature genes. **A** SVM-RFE analysis showing the 5-fold cross-validation accuracy against the number of features. **B** Lasso regression analysis plot of binomial deviance versus Log(λ). **C** RF feature importance ranking of genes based on the mean decrease in Gini coefficient with top-ranking genes including CTNNB1, APOE, and SLC1A3. **D** Venn diagram depicting the overlap of feature genes identified by SVM-RFE, Lasso, and RF methods. **E** Violin plots of expression levels of common feature genes between Con and COPD groups in the GSE76925 dataset. ***$p < 0.001$

(Fig. 7B). Calibration plot comparing the predicted and actual probabilities of COPD. The apparent and bias-corrected lines closely align with the ideal line, demonstrating that the nomogram model provides reliable predictions (Fig. 7C). DCA illustrates the clinical utility of the nomogram. The net benefit, as shown by the blue line, suggests that using the nomogram to predict COPD risk provides a higher net benefit across a wide range of risk thresholds compared to treating all patients (red line) or none (green line) (Fig. 7D). These results suggest that the constructed nomogram, based on benzo(a)pyrene exposure-related feature genes, is a robust and reliable tool for predicting COPD risk, with high diagnostic accuracy and clinical utility.

Construction of an ANN model

Figure 8A depicts the architecture of the ANN model, which includes input nodes corresponding to the seven feature genes, hidden layers, and an output node for the classification of the patient group. The model's performance was evaluated using ROC curves for both the training set and the validation set. In the training set (Fig. 8B), the ANN model achieved an AUC of 0.973, indicating excellent classification performance. For the validation set (Fig. 8C), the AUC was 0.812, demonstrating robust performance in an independent dataset. These results suggest that the identified feature genes and the constructed ANN model provide a reliable method for distinguishing COPD patients based on benzo(a)pyrene exposure, potentially aiding in the early diagnosis and targeted treatment of COPD.

Molecular docking evaluation of benzo(a)pyrene with proteins encoded by 7 feature genes

Molecular docking was conducted to evaluate the binding affinity of benzo(a)pyrene with proteins encoded by the seven identified feature genes. The Vina scores, which represent the binding affinities, were measured for each protein-benzo(a)pyrene complex. Notably, the docking score for benzo(a)pyrene with CDK1 was the lowest at -12.3, indicating the strongest binding affinity among the evaluated proteins (Fig. 9A). Other significant

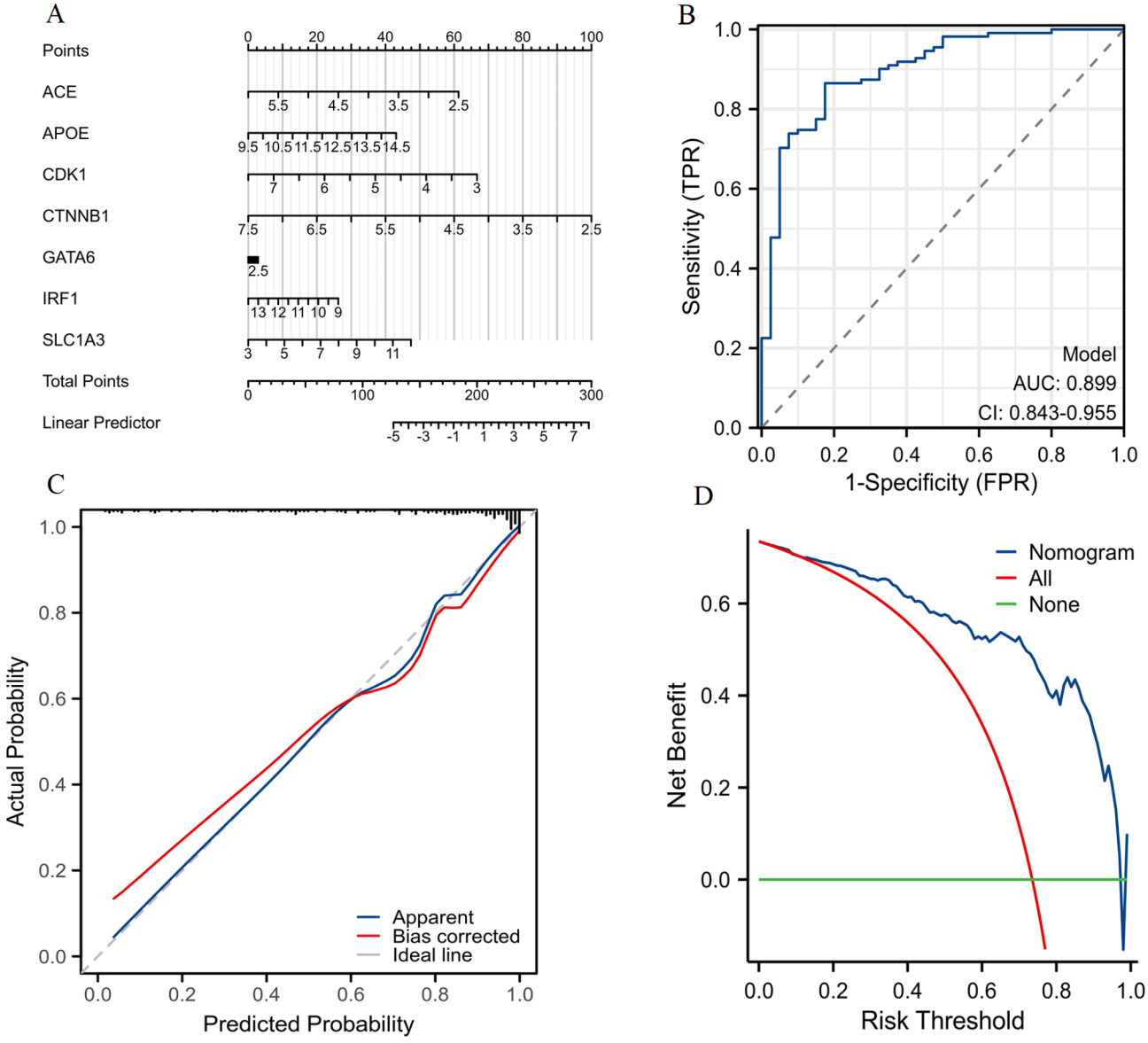

Fig. 7 Construction and validation of a nomogram. **A** Nomogram constructed using the expression levels of seven feature genes to predict COPD risk. Each gene's expression level is assigned a score, which sums to produce the total points and corresponding linear predictor. **B** ROC curve of the nomogram model. **C** Calibration plot comparing predicted probabilities versus actual probabilities of COPD risk. **D** DCA illustrating net benefit across different risk thresholds

binding affinities were observed with ACE (-9.6), APOE (-7.3), CTNNB1 (-6.5), GATA6 (-8.3), IRF1 (-6.7), and SLC1A3 (-8.8). The molecular surface structure of CDK1, highlighting the docking region where benzo(a)pyrene binds (Fig. 9B). A detailed view of the docking interaction between benzo(a)pyrene and CDK1, illustrating the binding pocket and key interacting residues (Fig. 9C). These findings suggest that CDK1, among other feature gene-related proteins, has the highest binding affinity to benzo(a)pyrene, which may play a crucial role in the molecular mechanisms underlying COPD induced by benzo(a)pyrene exposure.

Discussion

BaP, a polycyclic aromatic hydrocarbon, is a well-known environmental pollutant that has been implicated in various respiratory diseases [15, 16]. The relationship between BaP exposure and the pathogenesis of COPD is of significant concern, as BaP is known to induce oxidative stress and inflammation, both of which are critical components in the development and progression of COPD. Understanding the molecular mechanisms by which BaP influences these pathways is essential for identifying potential therapeutic targets and biomarkers for COPD.

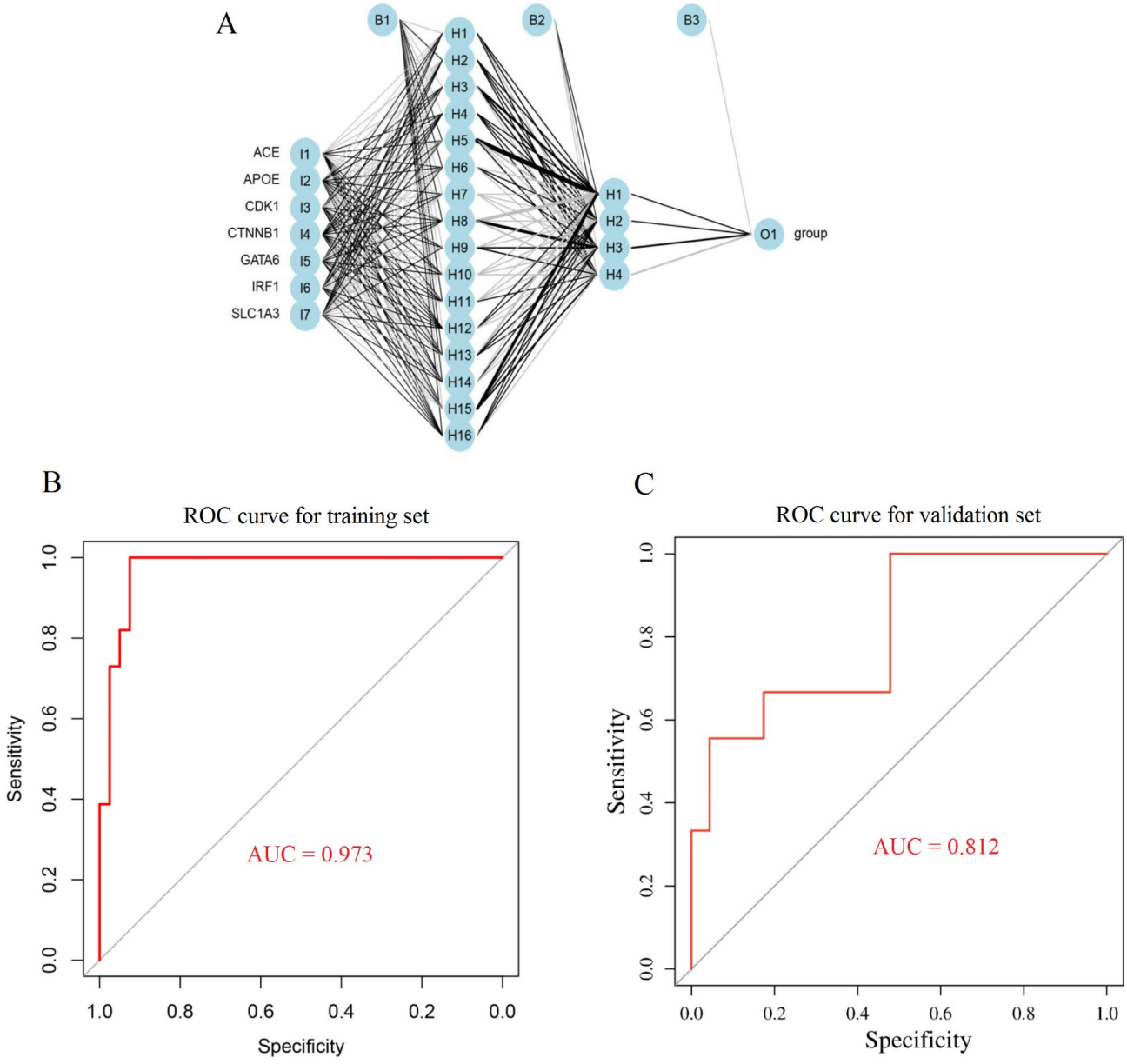

Fig. 8 Construction of an ANN model. **A** The architecture of the ANN model, constructed based on the expression profiles of seven identified feature genes (ACE, APOE, CDK1, CTNNB1, GATA6, IRF1, and SLC1A3). **B** ROC curve for the training set. **C** ROC curve for the validation set

Our research underscores the essential role of oxidative stress and inflammatory signaling pathways in the toxic effects of BaP exposure in individuals with COPD. Through functional enrichment analysis, we identified significant pathways involved, including the response to reactive oxygen species, TNF signaling pathway, C-type lectin receptor signaling pathway, and FoxO signaling pathway, underscores the intricate molecular mechanisms through which BaP exacerbates COPD pathology. These pathways are not only pivotal for understanding the immediate cellular responses to environmental toxins but also provide potential therapeutic targets for mitigating the adverse effects of BaP in COPD patients. Oxidative stress is a central factor in the progression of COPD and has been shown to contribute significantly to lung inflammation and tissue damage in response to environmental pollutants [8, 17, 18]. BaP, a potent polycyclic aromatic hydrocarbon, is metabolized to reactive intermediates that generate ROS, leading to cellular damage and the activation of stress response pathways [19, 20]. Our analysis revealed the enrichment of pathways involved in ROS response, which is consistent with previous studies demonstrating that BaP exposure induces oxidative stress, triggering inflammatory cascades and cellular apoptosis in lung diseases [21–23]. In COPD, this heightened oxidative environment accelerates the

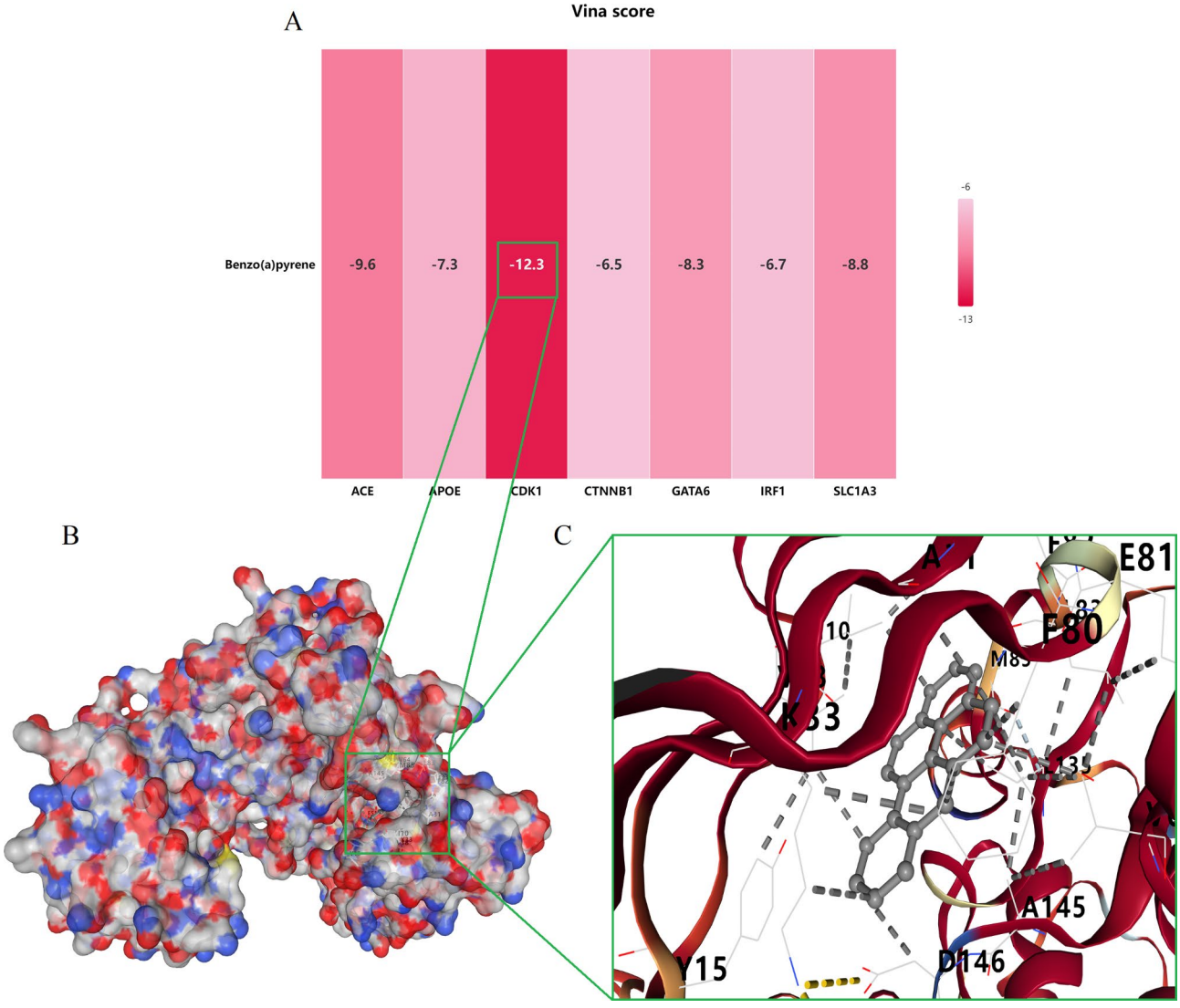

Fig. 9 Molecular docking analysis. **A** Heatmap of vina scores representing the binding affinities of benzo(a)pyrene with proteins encoded by the feature genes. **B** Molecular surface representation of the CDK1 protein, showing the overall structure and the docking region for benzo(a)pyrene. **C** Magnified view of the binding interaction between benzo(a)pyrene and the CDK1 protein, highlighting the binding pocket and key interacting residues

degradation of lung tissue and exacerbates airflow limitation [24, 25]. Targeting oxidative stress pathways could offer a promising avenue for therapeutic interventions aimed at reducing lung injury in COPD patients exposed to environmental pollutants. The TNF signaling pathway is a well-established mediator of inflammation and is critical in the pathogenesis of both COPD and BaP toxicity [26–28]. Previous studies have shown that BaP exposure increases TNF-α levels, which in turn activates downstream inflammatory cytokines, contributing to a pro-inflammatory microenvironment in the lungs [29–31]. In COPD, the chronic activation of the TNF pathway is associated with the recruitment of immune cells, increased mucus production, and the destruction of alveolar structures [32–35]. Our results support these findings, suggesting that BaP-induced TNF signaling plays a pivotal role in exacerbating COPD-related inflammation and tissue damage. Thus, therapeutic modulation of TNF signaling may help attenuate the inflammatory burden in individuals with COPD exposed to BaP. The C-type lectin receptors (CLRs) signaling pathway is integral to the recognition of pathogens and the modulation of immune responses [36]. Recent studies have highlighted the role of CLRs in regulating inflammation, particularly in the context of environmental pollutants [37, 38]. In lung diseases, CLRs may engage with diverse immune cell populations during the mechanisms of tissue injury and subsequent repair processes [39]. BaP, through its interaction with various immune receptors, may activate CLR pathways, which could further amplify the inflammatory response in the lungs of COPD patients [40, 41]. This connection between environmental toxins and immune

receptor signaling suggests that targeting CLR-mediated inflammation could provide a novel approach for reducing the effects of BaP exposure in COPD. FoxO transcription factors are key regulators of cellular responses to oxidative stress, apoptosis, and inflammation. FoxO signaling has been linked to the regulation of various inflammatory cytokines and cell survival pathways, with relevance to chronic diseases like COPD [42–44]. In our study, we observed that BaP exposure led to the activation of FoxO signaling, which may contribute to the regulation of genes involved in inflammation and cellular survival under oxidative stress. Therefore, the activation of FoxO signaling in response to BaP may represent a protective mechanism that attempts to restore cellular homeostasis, but if dysregulated, it could further exacerbate the pathogenesis of COPD.

Moreover, our assessment of immune cell infiltration using ssGSEA revealed substantial alterations in the immune landscape of COPD patients compared to healthy controls. The significant increase in the infiltration levels of various immune cell types, including macrophages and T cells, aligns with findings from other studies that have reported immune dysregulation in COPD. The heightened presence of macrophages, suggests a shift towards a pro-inflammatory phenotype that may contribute to tissue damage and airway remodeling in COPD patients [45, 46]. These macrophages are known to produce a variety of inflammatory cytokines and chemokines, which can further recruit additional immune cells and perpetuate the inflammatory cycle, ultimately leading to exacerbated symptoms and disease progression. Additionally, the increased infiltration of T cells, especially T helper cells and TFH, highlights the role of adaptive immunity in COPD. Studies have shown that these T cells may contribute to epithelial cell apoptosis and chronic inflammation [47, 48]. The interplay between innate and adaptive immune responses is complex, as activated T cells can also influence macrophage function, thereby sustaining the inflammatory milieu [35, 49]. This reciprocal activation reinforces the notion that targeting specific immune pathways could be beneficial for managing COPD. The correlation between oxidative stress and immune cell infiltration is noteworthy. Oxidative stress, which is often exacerbated by environmental factors such as cigarette smoke and air pollution, can modify the behavior of immune cells, promoting a pro-inflammatory phenotype [50–52]. This suggests that oxidative stress is not merely a consequence of inflammation but rather a driving factor that shapes the immune landscape in COPD [53, 54]. Therefore, strategies aimed at reducing oxidative stress, such as the use of antioxidants or other pharmacological interventions, could potentially alter the immune response, reduce inflammation, and improve clinical outcomes in COPD patients [55].

The identification of feature genes associated with BaP exposure using machine learning techniques provides a novel approach to understanding the molecular mechanisms underlying COPD. The common set of seven feature genes (ACE, APOE, CDK1, CTNNB1, GATA6, IRF1, and SLC1A3) identified in our study has not only shown significant expression differences between COPD and control groups but also highlights their potential as biomarkers for BaP exposure. Previous research has indicated that these genes are involved in various biological processes, including inflammation and cellular stress responses [56–60]. The robustness of these feature genes, as demonstrated by our machine learning analyses, supports their relevance in the context of COPD and BaP exposure. The construction of a nomogram for predicting COPD risk based on the expression profiles of the identified feature genes represents a significant advancement in the field. The high diagnostic accuracy of the nomogram suggests its potential utility in clinical settings for identifying individuals at risk of developing COPD due to BaP exposure. This aligns with the growing emphasis on personalized medicine, where risk assessment tools can guide preventive strategies and therapeutic interventions [61]. Furthermore, our molecular docking studies revealed that CDK1 exhibits the strongest binding affinity to BaP among the identified feature genes. This finding is particularly intriguing, as CDK1 is known to play a crucial role in cell cycle regulation and has been implicated in various cancers and inflammatory diseases [58, 62]. The interaction between BaP and CDK1 may provide insights into the molecular mechanisms by which BaP exposure contributes to COPD pathogenesis, warranting further investigation into the role of CDK1 in this context.

Conclusions

In conclusion, our study elucidates the complex interplay between BaP exposure, oxidative stress, inflammation, and immune cell infiltration in the pathogenesis of COPD. The identification of key feature genes and the development of a predictive nomogram offer promising avenues for future research and clinical application. As we continue to explore the molecular underpinnings of COPD, it is imperative to consider the broader implications of environmental pollutants like BaP on respiratory health. Future studies should aim to validate our findings in larger cohorts and investigate the therapeutic potential of targeting the identified pathways and genes in COPD management.

Supplementary Information

The online version contains supplementary material available at https://doi.org/10.1186/s40360-025-00842-1 .

Supplementary Material 1

Supplementary Material 2

Acknowledgements
Not applicable.

Author contributions
Jiehua Deng, Yongyu Chen, and Xiaofeng Li wrote the manuscript. Hui Zhang, Xuan Wei, Xin Feng, Xue Qiu, and Bin Liang analyzed the data and produced the figures. Lixia Wei and Jianquan Zhang reviewed and edited the manuscript. All authors reviewed the manuscript.

Funding
This work was supported by grants from the Natural Science Foundation of Guangdong Province (2024A1515011073), the Natural Science Foundation of Guangdong Province (2023A1515012987), the Shenzhen Science Technology Program (JCYJ 20230807110914029), the Futian Healthcare Research Project (FTWS2022019), the Key clinical specialty of Shenzhen Futian District (QZDZK-202406), Guangxi Young and Middle aged Teacher's Basic Ability Promoting Project (2023KY0121), the Science and Technology Department of Guangxi Zhuang Autonomous Foundation of Guangxi Key Research and Development Program (2024AB17061), the Futian Healthcare Research Project (FTWS2021055), the Beijing Norman Bethune Public Welfare Foundation, horizontal BJ-RW2020022J.

Data availability
The data utilized in this study were sourced from the GEO database, accessible at https://www.ncbi.nlm.nih.gov/geo/.

Declarations

Ethics approval and consent to participate
Not applicable.

Consent for publication
Not applicable.

Competing interests
The authors declare no competing interests.

Author details
[1]Department of Respiratory and Critical Medicine, The Eighth Affiliated Hospital, Sun Yat-sen University, 3025 Shennan Zhong Lu, Shenzhen City, Guangdong Province 518033, China
[2]Department of Cardiology, The First Affiliated Hospital of Guangxi Medical University, Nanning 530021, China
[3]Department of Hematology, The First Affiliated Hospital of Guangxi Medical University, Nanning 530021, China
[4]Department of Respiratory and Critical Medicine, The First Affiliated Hospital of Guangxi Medical University, Nanning 530021, China
[5]Gastroenterology and Respiratory Internal Medicine Department, The Afliated Tumor Hospital of Guangxi Medical University, Nanning 530021, China
[6]Department of Gastroenterology, The First Affiliated Hospital of Guangxi Medical University, Nanning 530021, China

Received: 14 November 2024 / Accepted: 15 January 2025
Published online: 17 February 2025

References

1. Labaki WW, Rosenberg SR. Chronic obstructive Pulmonary Disease. Ann Intern Med. 2020;173:Itc17–32.
2. Vogelmeier CF, Román-Rodríguez M, Singh D, Han MK, Rodríguez-Roisin R, Ferguson GT. Goals of COPD treatment: focus on symptoms and exacerbations. Respir Med. 2020;166:105938.
3. Raherison C, Girodet PO. Epidemiology of COPD. Eur Respiratory Review: Official J Eur Respiratory Soc. 2009;18:213–21.
4. Bagdonas E, Raudoniute J, Bruzauskaite I, Aldonyte R. Novel aspects of pathogenesis and regeneration mechanisms in COPD. Int J Chronic Obstr Pulm Dis. 2015;10:995–1013.
5. Peng K, Li Z, Gao TR, Lv J, Wang WJ, Zhan P, Yao WC, Zhao H, Wang H, Xu DX, Huang Y, Tan ZX. Polycyclic aromatic hydrocarbon exposure burden: individual and mixture analyses of associations with chronic obstructive pulmonary disease risk. Environ Res. 2023;222:115334.
6. Bukowska B, Mokra K, Michałowicz J. Benzo[a]pyrene-Environmental occurrence, human exposure, and mechanisms of toxicity. Int J Mol Sci 23:2022.
7. Pauk N, Klimesova S, Kara J, Topinka J, Labaj J. The relevance of monitoring of antibodies against the polycyclic aromatic hydrocarbon (PAH) and PAH-DNA adducts in serum in relation to lung cancer and chronic obstructive pulmonary disease (COPD). Neoplasma. 2013;60:182–7.
8. Wang Q, Liu S. The effects and Pathogenesis of PM2.5 and its components on Chronic Obstructive Pulmonary Disease. Int J Chronic Obstr Pulm Dis. 2023;18:493–506.
9. Wen L, Ben X, Yang Z, Wu Y, Tan Y, Chen Q, Liang H, Li Y, Wu X, Liu S, Weng X, Tian D, Jing C. Association between co-exposure of polycyclic aromatic hydrocarbons and chronic obstructive pulmonary disease among the US adults: results from the 2013–2016 National Health and Nutrition Examination Survey. Environ Sci Pollut Res Int. 2023;30:62981–92.
10. Kumar A, Sinha N, Kodidela S, Zhou L, Singh UP, Kumar S. Effect of benzo(a) pyrene on oxidative stress and inflammatory mediators in astrocytes and HIV-infected macrophages. PLoS ONE. 2022;17:e0275874.
11. Estrago-Franco MF, Moustafa MT, Riazi-Esfahani M, Sapkal AU, Piche-Lopez R, Patil AJ, Sharma A, Falatoonzadeh P, Chwa M, Luczy-Bachman G, Kuppermann BD, Kenney MC. Effects of Benzo(e)pyrene on Reactive Oxygen/Nitrogen Species and inflammatory cytokines induction in human RPE cells and attenuation by mitochondrial-involved mechanism. J Ophthalmic Vis Res. 2016;11:385–93.
12. Qi W, Liu L, Zeng Q, Zhou Z, Chen D, He B, Gong S, Gao L, Wang X, Xiong J, Cai D, Yu S, Zhao L. Contribution of cuproptosis and Cu metabolism-associated genes to chronic obstructive pulmonary disease. J Cell Mol Med. 2023;27:4034–44.
13. Sun S, Shen Y, Wang J, Li J, Cao J, Zhang J. Identification and validation of Autophagy-related genes in Chronic Obstructive Pulmonary Disease. Int J Chronic Obstr Pulm Dis. 2021;16:67–78.
14. Bindea G, Mlecnik B, Tosolini M, Kirilovsky A, Waldner M, Obenauf AC, Angell H, Fredriksen T, Lafontaine L, Berger A, Bruneval P, Fridman WH, Becker C, Pagès F, Speicher MR, Trajanoski Z, Galon J. Spatiotemporal dynamics of intratumoral immune cells reveal the immune landscape in human cancer. Immunity. 2013;39:782–95.
15. Li MD, Chen LH, Xiang HX, Jiang YL, Lv BB, Xu DX, Zhao H, Fu L. Benzo[a] pyrene evokes epithelial-mesenchymal transition and pulmonary fibrosis through AhR-mediated Nrf2-p62 signaling. J Hazard Mater. 2024;473:134560.
16. Wang Z. Mechanisms of the synergistic lung tumorigenic effect of arsenic and benzo(a)pyrene combined- exposure. Sem Cancer Biol. 2021;76:156–62.
17. Yang W, Omaye ST. Air pollutants, oxidative stress and human health. Mutat Res. 2009;674:45–54.
18. Fang ZF, Fu Y, Peng Y, Song SR, Wang ZN, Yang Y, Nie YC, Han HL, Teng YB, Xiao WM, Chen JP, Zhou BJ, Ou GL, Xie JX, Liu XY, Zhang JJ, Zhong NS. Citrus peel extract protects against diesel exhaust particle-induced chronic obstructive pulmonary disease-like lung lesions and oxidative stress. Food Funct. 2023;14:9841–56.
19. Qiu L, Chen X, Guo B, Liao Z, Buttino I, Yan X, Qi P. Unraveling the protective role of Nrf2 in molluscs: insights into mitochondrial and apoptosis pathways in the defense against Bap-induced oxidative stress. Aquat Toxicol. 2023;264:106728.
20. Bukowska B, Duchnowicz P. Molecular mechanisms of action of selected substances involved in the reduction of benzo[a]pyrene-induced oxidative stress. Molecules 27:2022.
21. Ni Z, Ma H, Li X, Zou L, Liu Z, Wang X, Ma H, Yang L. Wogonin alleviates BaP-induced DNA damage and oxidative stress in human airway epithelial cells by dual inhibiting CYP1A1 activity and expression. Environ Toxicol. 2023;38:2717–29.
22. Yeo CD, Kim JW, Ha JH, Kim SJ, Lee SH, Kim IK, Kim YK. Chemopreventive effect of phosphodieasterase-4 inhibition in benzo(a)pyrene-induced murine lung cancer model. Exp Lung Res. 2014;40:500–6.
23. Min L, He S, Chen Q, Peng F, Peng H, Xie M. Comparative proteomic analysis of cellular response of human airway epithelial cells (A549) to benzo(a) pyrene. Toxicol Mech Methods. 2011;21:374–82.

24. Tan WSD, Liao W, Peh HY, Vila M, Dong J, Shen HM, Wong WSF. Andrographolide simultaneously augments Nrf2 antioxidant defense and facilitates autophagic flux blockade in cigarette smoke-exposed human bronchial epithelial cells. Toxicol Appl Pharmcol. 2018;360:120–30.
25. Hirai DM, Jones JH, Zelt JT, da Silva ML, Bentley RF, Edgett BA, Gurd BJ, Tschakovsky ME, O'Donnell DE, Neder JA. Oral N-acetylcysteine and exercise tolerance in mild chronic obstructive pulmonary disease. J Appl Physiol (Bethesda Md: 1985). 2017;122:1351–61.
26. Racanelli AC, Kikkers SA, Choi AMK, Cloonan SM. Autophagy and inflammation in chronic respiratory disease. Autophagy. 2018;14:221–32.
27. Ouyang W, Hu Y, Li J, Ding M, Lu Y, Zhang D, Yan Y, Song L, Qu Q, Desai D, Amin S, Huang C. Direct evidence for the critical role of NFAT3 in benzo[a] pyrene diol-epoxide-induced cell transformation through mediation of inflammatory cytokine TNF induction in mouse epidermal Cl41 cells. Carcinogenesis. 2007;28:2218–26.
28. Shahid A, Ali R, Ali N, Hasan SK, Rashid S, Majed F, Sultana S. Attenuation of genotoxicity, oxidative stress, apoptosis and inflammation by rutin in benzo(a)pyrene exposed lungs of mice: plausible role of NF-κB, TNF-α and Bcl-2. J Complement Integr Med. 2016;13:17–29.
29. You M, Song Y, Chen J, Liu Y, Chen W, Cen Y, Zhao X, Tao Z, Yang G. Combined exposure to benzo(a)pyrene and dibutyl phthalate aggravates pro-inflammatory macrophage polarization in spleen via pyroptosis involving cathepsin B. Sci Total Environ. 2023;881:163460.
30. Almatroodi SA, Alrumaihi F, Alsahli MA, Alhommrani MF, Khan A, Rahmani AH. Curcumin, an active constituent of Turmeric spice: implication in the Prevention of Lung Injury Induced by Benzo(a) pyrene (BaP) in rats. Molecules 25:2020.
31. Shahid A, Ali R, Ali N, Kazim Hasan S, Barnwal P, Mohammad Afzal S, Vafa A, Sultana S. Methanolic bark extract of Acacia catechu ameliorates benzo(a) pyrene induced lung toxicity by abrogation of oxidative stress, inflammation, and apoptosis in mice. Environ Toxicol. 2017;32:1566–77.
32. Huang AX, Lu LW, Liu WJ, Huang M. Plasma inflammatory cytokine IL-4, IL-8, IL-10, and TNF-α levels correlate with pulmonary function in patients with Asthma-Chronic Obstructive Pulmonary Disease (COPD) Overlap Syndrome. Med Sci Monitor: Int Med J Experimental Clin Res. 2016;22:2800–8.
33. Li S, Zhao S, Wu Z, Wang F, Li W. Alteration of immune profiles is associated with pulmonary function and symptoms in patients with chronic obstructive pulmonary disease. Mol Med Rep 24:2021.
34. Peres A, Dorneles GP, Dias AS, Vianna P, Chies JAB, Monteiro MB. T-cell profile and systemic cytokine levels in overweight-obese patients with moderate to very-severe COPD. Respir Physiol Neurobiol. 2018;247:74–9.
35. Gadgil A, Duncan SR. Role of T-lymphocytes and pro-inflammatory mediators in the pathogenesis of chronic obstructive pulmonary disease. Int J Chronic Obstr Pulm Dis. 2008;3:531–41.
36. Angelina A, Martín-Cruz L, de la Rocha-Muñoz A, Lavín-Plaza B, Palomares O. C-Type lectin receptor mediated Modulation of T2 Immune responses to Allergens. Curr Allergy Asthma Rep. 2023;23:141–51.
37. Ciencewicki JM, Verhein KC, Gerrish K, McCaw ZR, Li J, Bushel PR, Kleeberger SR. Effects of mannose-binding lectin on pulmonary gene expression and innate immune inflammatory response to ozone. Am J Physiol Lung Cell Mol Physiol. 2016;311:L280–91.
38. Peters K, Peters M. The role of Lectin Receptors and their ligands in Controlling allergic inflammation. Front Immunol. 2021;12:635411.
39. Effendi WI, Nagano T, Hasan H, Yudhawati R. Immunoregulatory Property of C-Type Lectin-Like Receptors in Fibrosing interstitial lung diseases. Int J Mol Sci 21:2020.
40. Su W, Zha S, Wang Y, Shi W, Xiao G, Chai X, Wu H, Liu G. Benzo[a]pyrene exposure under future ocean acidification scenarios weakens the immune responses of blood clam, Tegillarca Granosa. Fish Shellfish Immunol. 2017;63:465–70.
41. Sparfel L, Pinel-Marie ML, Boize M, Koscielny S, Desmots S, Pery A, Fardel O. Transcriptional signature of human macrophages exposed to the environmental contaminant benzo(a)pyrene. Toxicol Sci. 2010;114:247–59.
42. Mumby S, Adcock IM. Recent evidence from omic analysis for redox signalling and mitochondrial oxidative stress in COPD. J Inflamm (London England). 2022;19:10.
43. Puig-Vilanova E, Rodriguez DA, Lloreta J, Ausin P, Pascual-Guardia S, Broquetas J, Roca J, Gea J, Barreiro E. Oxidative stress, redox signaling pathways, and autophagy in cachectic muscles of male patients with advanced COPD and lung cancer. Free Radic Biol Med. 2015;79:91–108.
44. Hwang JW, Rajendrasozhan S, Yao H, Chung S, Sundar IK, Huyck HL, Pryhuber GS, Kinnula VL, Rahman I. FOXO3 deficiency leads to increased susceptibility to cigarette smoke-induced inflammation, airspace enlargement, and chronic obstructive pulmonary disease. J Immunol (Baltimore Md: 1950). 2011;187:987–98.
45. Tetley TD. Macrophages and the pathogenesis of COPD. Chest. 2002;121:s156–9.
46. He S, Xie L, Lu J, Sun S. Characteristics and potential role of M2 macrophages in COPD. Int J Chronic Obstr Pulm Dis. 2017;12:3029–39.
47. Huber ME, Larson E, Lust TN, Heisler CM, Harriff MJ. Chronic obstructive pulmonary disease and cigarette smoke lead to Dysregulated Mucosal-associated invariant T-Cell activation. Am J Respir Cell Mol Biol. 2023;68:90–102.
48. Huang S, He Q, Zhou L. T cell responses in respiratory viral infections and chronic obstructive pulmonary disease. Chin Med J. 2021;134:1522–34.
49. Booth S, Hsieh A, Mostaco-Guidolin L, Koo HK, Wu K, Aminazadeh F, Yang CX, Quail D, Wei Y, Cooper JD, Paré PD, Hogg JC, Vasilescu DM, Hackett TL. A single-cell atlas of small Airway Disease in Chronic Obstructive Pulmonary Disease: a cross-sectional study. Am J Respir Crit Care Med. 2023;208:472–86.
50. Xie S, Wang X. CRYAB reduces cigarette smoke-induced inflammation, apoptosis, and oxidative stress by retarding PI3K/Akt and NF-κB signaling pathways in human bronchial epithelial cells. Allergol Immunopathol. 2022;50:23–9.
51. Pace E, Ferraro M, Di Vincenzo S, Gerbino S, Bruno A, Lanata L, Gjomarkaj M. Oxidative stress and innate immunity responses in cigarette smoke stimulated nasal epithelial cells. Toxicol vitro: Int J Published Association BIBRA. 2014;28:292–9.
52. Muthumalage T, Pritsos K, Hunter K, Pritsos C. Commonly used air filters fail to eliminate secondhand smoke induced oxidative stress and inflammatory responses. Toxicol Mech Methods. 2017;27:458–66.
53. Domej W, Oettl K, Renner W. Oxidative stress and free radicals in COPD–implications and relevance for treatment. Int J Chronic Obstr Pulm Dis. 2014;9:1207–24.
54. Finicelli M, Digilio FA, Galderisi U, Peluso G. The emerging role of macrophages in Chronic Obstructive Pulmonary Disease: the potential impact of oxidative stress and Extracellular Vesicle on Macrophage polarization and function. Antioxid (Basel Switzerland) 11:2022.
55. Kirkham P, Rahman I. Oxidative stress in asthma and COPD: antioxidants as a therapeutic strategy. Pharmacol Ther. 2006;111:476–94.
56. Cao DY, Spivia WR, Veiras LC, Khan Z, Peng Z, Jones AE, Bernstein EA, Saito S, Okwan-Duodu D, Parker SJ, Giani JF, Divakaruni AS, Van Eyk JE, Bernstein KE. ACE overexpression in myeloid cells increases oxidative metabolism and cellular ATP. J Biol Chem. 2020;295:1369–84.
57. Dose J, Huebbe P, Nebel A, Rimbach G. APOE genotype and stress response - a mini review. Lipids Health Dis. 2016;15:121.
58. Zhu S, Al-Mathkour M, Cao L, Khalafi S, Chen Z, Poveda J, Peng D, Lu H, Soutto M, Hu T, McDonald OG, Zaika A. El-Rifai, CDK1 bridges NF-κB and β-catenin signaling in response to H. Pylori infection in gastric tumorigenesis. Cell Rep. 2023;42:112005.
59. Toyama T, Kudryashova TV, Ichihara A, Lenna S, Looney A, Shen Y, Jiang L, Teos L, Avolio T, Lin D, Kaplan U, Marden G, Dambal V, Goncharov D, Delisser H, Lafyatis R, Seta F, Goncharova EA, Trojanowska M. GATA6 coordinates cross-talk between BMP10 and oxidative stress axis in pulmonary arterial hypertension. Sci Rep. 2023;13:6593.
60. Li H, Chen X, Xu J, Zhu L, Li C, Sun X, Li X, Guo J, Li J, Wang S, He Y, Wang H, Huang C, Meng XM, Li J. GRP/GRPR enhances alcohol-associated liver injury through the IRF1-mediated Caspase-1 inflammasome and NOX2-dependent ROS pathway. Hepatology (Baltimore MD). 2024;79:392–408.
61. Oh S, Mok H, Jo K. Development and validation of a nomogram for predicting COPD: a nationwide population-based study in South Korea. Medicine. 2024;103:e39901.
62. Zhang J, Di Y, Zhang B, Li T, Li D, Zhang H. CDK1 and CCNA2 play important roles in oral squamous cell carcinoma. Medicine. 2024;103:e37831.

Publisher's note